Inorg. Chem. **2004**, *43*, 6334–6344

Thienyl Carboxylate Ligands Bound to and Bridging MM Quadruple Bonds, M = Mo or W: Models for Polythiophenes Incorporating MM Quadruple Bonds

Matthew J. Byrnes,[†] Malcolm H. Chisholm,*[,†] Robin J. H. Clark,*[,‡] Judith C. Gallucci,[†] Christopher M. Hadad,*[,†] and Nathan J. Patmore[†]

Department of Chemistry, The Ohio State University, 100 W. 18th Avenue, Columbus, Ohio 43210-1185, and Christopher Ingold Laboratories, University College London, 20 Gordon Street, London WC1H 0AJ, U.K.

Received June 29, 2004

A series of compounds of the form $[M_2L_4]$ and $[\{(^tBuCO_2)_3M_2\}_2(\mu\text{-}L')]$ have been made where M = Mo or W, L = a thienyl, bithienyl, or terthienyl carboxylate, and L′ = a corresponding thienyl dicarboxylate. The electronic absorption spectra are reported and the electronic structures discussed. Intense metal-to-ligand charge transfer bands traverse the visible and near-IR regions of the electronic absorption spectrum. The compounds show reversible metal-based oxidations and quasireversible ligand-based reductions. The molecular structure of $Mo_2(O_2C\text{-}2\text{-}Th)_4 \cdot 2THF$ is reported, on the basis of a single crystal X-ray diffraction study. These compounds provide insight into the expected properties of related dimetalated polythiophenes incorporating MM quadruple bonds.

Introduction

Conjugated organic polymers such as poly-*p*-phenylenes, poly-*p*-phenylene vinylenes, polypyrroles, and polythiophenes have attracted enormous attention over the past two decades.[1] These materials are natural semiconductors with tunable band gaps and may be doped so as to show significant conductivity as thin films. In addition, they are finding applications in the production of transistors, photovoltaics, photomagnetic materials, and light-emitting diodes. These organic light-emitting diodes, OLEDs, have already achieved a significant marketplace value. The introduction of metal ions into organic polymers offers potential in the area of inorganic−organic hybrid materials, and this fact has not gone unnoticed. Indeed, the incorporation of metal ions into conjugated organic polymers has its origin in work with polyalkynyl platinum(II) complexes[2] and 1,1′-polyferrocenes,[3] which dates back over three decades. Although much attention has been devoted to the study of the electrical conductivity of thin films in these types of materials, there have been systematic studies of other properties as can be seen from reports from the groups of Friend and Raithby who have studied the emissive properties of metalated conjugated polymers.[4−8]

Wolf has described that metalated conjugated polymers can be categorized into one of three classes.[9] These are pictorially represented in Scheme 1. Class A compounds contain the metal as a side-chain appendage that is electronically insulated from the backbone of the conjugated polymer, whereas in class B, the side-chain attachment allows for

* To whom correspondence should be addressed. E-mail: Chisholm@chemistry.ohio-state.edu.
† The Ohio State University.
‡ University College London.

(1) *Handbook of Conducting Polymers*, 2nd Ed.; Skotheim, T. A., Elsenbaumer, R. L., Reynolds, J. R., Eds.; 1997.
(2) Sonogashira, K.; Takahashi, S.; Hagihara, N. *Macromolecules* **1977**, *10*, 879.
(3) Nguyen, P.; Gomez-Elipe, P.; Manners, I. *Chem. Rev.* **1999**, *99*, 1515.
(4) Li, P.; Ahrens, B.; Choi, K.-H.; Khan, M. S.; Raithby, P. R.; Wilson, P. J.; Wong, W.-Y. *CrystEngComm* **2002**, *4*, 405.
(5) Khan, M. S.; Al-Mandhary, M. R. A.; Al-Suti, M. K.; Feeder, N.; Nahar, S.; Koehler, A.; Friend, R. H.; Wilson, P. J.; Raithby, P. R. *Dalton Trans.* **2002**, 2441.
(6) Younus, M.; Kohler, A.; Cron, S.; Chawdhury, N.; Al-Mandhary, M. R. A.; Khan, M. S.; Lewis, J.; Long, N. J.; Friend, R. H.; Raithby, P. R. *Angew. Chem., Int. Ed.* **1998**, *37*, 3036.
(7) Chawdhury, N.; Kohler, A.; Friend, R. H.; Wong, W. Y.; Lewis, J.; Younus, M.; Raithby, P. R.; Corcoran, T. C.; Al-Mandhary, M. R. A.; Khan, M. S. *J. Chem. Phys.* **1999**, *110*, 4963.
(8) Khan, M. S.; Al-Mandhary, M. R. A.; Al-Suti, M. K.; Corcoran, T. C.; Al-Mahrooqi, Y.; Attfield, J. P.; Feeder, N.; David, W. I. F.; Shankland, K.; Friend, R. H.; Koehler, A.; Marseglia, E. A.; Tedesco, E.; Tang, C. C.; Raithby, P. R.; Collings, J. C.; Roscoe, K. P.; Batsanov, A. S.; Stimson, L. M.; Marder, T. B. *New J. Chem.* **2003**, *27*, 140.
(9) Wolf, M. O. *Adv. Mater.* **2001**, *13*, 545.

10.1021/ic040086n CCC: $27.50
Published on Web 09/01/2004

Scheme 1

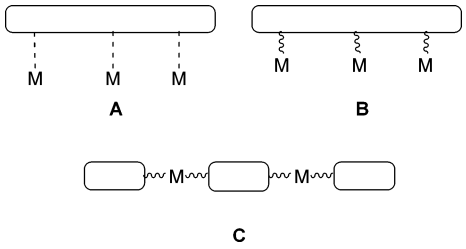

potential direct electronic communication. In class C, the metal is directly incorporated into the backbone of the conjugated polymer.

To date, the majority of work with metalated polymers has employed the later transition metals and lanthanides, and to our knowledge, no work has yet been done with dinuclear metal complexes containing MM multiple bonds. MM multiple bonded compounds display remarkable redox properties and may have a wide variety of electronic configurations for the MM bond.[10] These realizations led us to the present study wherein we have attached thienyl carboxylates to the MM quadruple bonds of molybdenum and tungsten as models for dimetalated polythiophenes incorporating MM quadruple bonds. The use of the carboxylate attachment was inspired by the recent studies of dicarboxylate bridged complexes $[M_2](\mu\text{-}O_2C-X\text{-}CO_2)[M_2]$ that have shown extensive electronic coupling of the two M_2 centers when X allows conjugation.[11−16] A preliminary report of some aspects of this work has appeared,[17] and an excellent review of metalated polythiophenes has just been published.[18]

Experimental Section

Physical Measurements. NMR spectra were recorded on a 400 MHz Bruker DPX Avance400 spectrometer. All ^{1}H NMR chemical shifts are reported in ppm relative to the protio impurity in THF-d_8 at 3.58 ppm or DMSO-d_6 at 2.09 ppm. Electronic spectra at room temperature were recorded using a Perkin-Elmer Lambda 900 spectrometer in THF solution. Variable temperature electronic spectra and X-band EPR spectra were recorded as previously reported.[13,14] Microanalyses were carried out by Atlantic Microlab, Inc. Cyclic voltammetric and differential pulse voltammetric data were collected with the aid of a Princeton Applied Research (PAR) 173A potentiostat−galvanostat equipped with a PAR 176 current-to-voltage converter with *iR* compensation capability. A single-compartment voltammetric cell was equipped with a platinum working electrode, a platinum wire auxiliary electrode, and a pseudoreference electrode consisting of a silver wire in 0.5 M ^{n}Bu$_4$NPF$_6$/THF separated from the bulk solution by a Vycor tip. Ferrocene was added as an internal reference and typically was found at +0.75 V under these conditions. Raman spectra were recorded using a Renishaw System 1000 and its associated He/Ne laser operating at 632.8 nm and argon ion laser operating at 514.5 nm. Samples of the 2,5-thienyl dicarboxylate bridged compounds were packed in capillaries and sealed under an inert atmosphere for the Raman spectra measurements.

Synthesis. All reactions were carried out under an atmosphere of oxygen-free UHP-grade argon using standard Schlenk techniques or under a dry and oxygen-free nitrogen atmosphere using standard glovebox techniques. All solvents were dried and degassed by standard methods and distilled prior to use. Ditungsten tetrapivalate,[19] dimolybdenum tetrapivalate,[20] 2,2′-bithiophene-5-carboxylic acid (2,2′-BThCO_2H), (2,2′:5′,2″-terthiophene)-5-dicarboxylic acid (2,2″-TThCO_2H), 2,2′-bithiophene-5,5′-dicarboxylic acid [2,2′-BTh$(CO_2H)_2$],[21] and (2,2′:5′,2″-terthiophene)-5,5″-dicarboxylic acid [2,5″-TTh$(CO_2H)_2$][22] were prepared according to the literature procedures. 2-Thienylcarboxylic acid, 3-thienylcarboxylic acid, 2,5-thienyldicarboxylic acid, 2,2′-bithiophene, 3-(2-thienyl)acrylic acid, and [Ni(dppp)Cl$_2$] (dppp = diphenylphosphinopropane) were purchased from commercial sources and used as received. [Mo$(CO)_6$] was purchased from Strem and used as received. *n*-Butyllithium (2.5 M in hexanes) was purchased from Acros and used as received.

[Mo$_2$(2-ThCO$_2$)$_4$]. [Mo$(CO)_6$] (2.00 g, 7.58 mmol) and 2-ThCO$_2$H (2.91 g, 22.7 mmol) were dissolved in a mixture of 1,2-dichlorobenzene (ca. 100 cm^3) and THF (ca. 50 cm^3) in a Schlenk flask fitted with a reflux condenser. The solution was then heated to ca. 140 °C for 16 h during which time an orange solution had formed. After the solution was allowed to cool slowly to room temperature, an orange solid precipitated, and the mother liquor was carefully decanted from this solid. The solid (1.82 g, 94% yield) was washed twice with hexanes (ca. 40 cm^3) and then dried in vacuo for 4 h.

Microanalysis found: C 34.34, H 1.69%. $C_{20}H_{12}O_8S_4Mo_2$ requires: C 34.30, H 1.73%. NMR (THF-d_8): δ_H (400 MHz) 7.81 (4H, dd, J_{HH} = 3.7 and 1.3 Hz), 7.57 (4H, dd, J_{HH} = 5.0 and 1.3 Hz), 7.10 (4H, dd, J_{HH} = 5.0 and 3.7 Hz). MALDI-MS: 700 (100 %, M$^+$).

[Mo$_2$(3-ThCO$_2$)$_4$]. The reaction was performed under similar conditions to those described for the preparation of [Mo$_2$(2-ThCO$_2$)$_4$] using 2.00 g of [Mo$(CO)_6$] (7.58 mmol) and 2.91 g of 3-ThCO$_2$H (22.7 mmol). A yellow solid was isolated from cooling the yellow solution to room temperature. The isolated solid (1.01 g, 38% yield) was washed twice with hexanes (ca. 40 cm^3) and then dried in vacuo for 4 h. This solid was virtually insoluble in THF.

Alternatively, 500 mg of [Mo$_2$(O$_2$C^{t}Bu)$_4$] (0.839 mmol) was dissolved in THF (ca. 10 cm^3) to form a clear yellow solution. To this solution was added 435 mg of 3-ThCO$_2$H (3.394 mmol), and an orange solution formed almost immediately. After ca. 5 min, a yellow solid was observed. The reaction was stirred for ca. 12 h before being stripped to dryness and washed with toluene (2 × 10 cm^3) and then hexanes (2 × 10 cm^3) to afford a bright yellow solid (430 mg, 73% yield) that was virtually insoluble in THF.

(10) Cotton, F. A.; Walton, R. A. *Multiple Bonds Between Metal Atoms*, 2nd ed.; Oxford University Press: Oxford, 1993.
(11) Cayton, R. H.; Chisholm, M. H.; Huffman, J. C.; Lobkovsky, E. B. *J. Am. Chem. Soc.* **1991**, *113*, 8709.
(12) Bursten, B. E.; Chisholm, M. H.; Hadad, C. M.; Li, J.; Wilson, P. J. *Chem. Commun.* **2001**, 2382.
(13) Bursten, B. E.; Chisholm, M. H.; Clark, R. J. H.; Firth, S.; Hadad, C. M.; MacIntosh, A. M.; Wilson, P. J.; Woodward, P. M.; Zaleski, J. M. *J. Am. Chem. Soc.* **2002**, *124*, 3050.
(14) Bursten, B. E.; Chisholm, M. H.; Clark, R. J. H.; Firth, S.; Hadad, C. M.; Wilson, P. J.; Woodward, P. M.; Zaleski, J. M. *J. Am. Chem. Soc.* **2002**, *124*, 12244.
(15) Chisholm, M. H.; Pate, B. D.; Wilson, P. J.; Zaleski, J. M. *Chem. Commun.* **2002**, 1084.
(16) Cotton, F. A.; Donahue, J. P.; Murillo, C. A. *J. Am. Chem. Soc.* **2003**, *125*, 5436.
(17) Byrnes, M. J.; Chisholm, M. H. *Chem. Commun.* **2002**, 2040.
(18) Stott, T. L.; Wolf, M. O. *Coord. Chem. Rev.* **2003**, *246*, 89.
(19) Santure, D. J.; Huffman, J. C.; Sattelberger, A. P. *Inorg. Chem.* **1985**, *24*, 371.
(20) Brignole, A. B.; Cotton, F. A. *Inorg. Synth.* **1971**, *13*, 81.
(21) Wang, S.; Brisse, F. *Macromolecules* **1998**, *31*, 2265.
(22) Liu, P.; Nakano, H.; Shirota, Y. *Liq. Cryst.* **2001**, *28*, 581.

Microanalysis found: C 34.30, H 1.66%. $C_{20}H_{12}O_8S_4Mo_2$ requires: C 34.30, H 1.73%. MALDI-MS: 702 (100 %, M^+).

[Mo_2(2,2′-BThCO_2)$_4$]. The reaction was performed under similar conditions to those described for the preparation of [Mo_2(2-ThCO_2)$_4$] using 0.42 g of [Mo(CO)$_6$] (1.58 mmol) and 1.0 g of 2,2′-BThCO_2H (4.76 mmol). A red solid was isolated from the now red solution after having been cooled to room temperature. The isolated solid (0.76 g, 93% yield) was recrystallized from THF layered with hexanes and then dried in vacuo for 4 h.

Microanalysis found: C 42.74, H 2.22%. $C_{36}H_{20}O_8S_8Mo_2$ requires: C 42.02, H 1.94%. NMR (THF-d_8): δ_H (400 MHz) 7.74 (4H, d, J_{HH} = 6.2 Hz), 7.38 (4H, d, J_{HH} = 8.1 Hz), 7.32 (4H, d, J_{HH} = 5.6 Hz), 7.25 (4H, d, J_{HH} = 6.2 Hz), 7.03 (4H, dd, J_{HH} = 6.9 and 6.9 Hz). MALDI-MS: 1029 (100 %, M^+).

[W_2(2-ThCO_2)$_4$]. [W_2(O_2C^tBu)$_4$] (119 mg, 0.154 mmol) was dissolved in toluene (ca. 15 cm^3) in a Schlenk flask, and to this clear yellow solution was added 2-ThCO_2H (79 mg, 0.616 mmol). The color changed immediately to a deep purple, and this solution was then stirred for 3 days at room temperature. This deep purple solid was filtered and then washed with toluene and then hexanes before being dried in vacuo.

Microanalysis found: C 25.70, H 1.87%. $C_{20}H_{12}O_8S_4W_2$ requires: C 27.42, H 1.87%. NMR (THF-d_8): δ_H (400 MHz) 7.72 (4H, dd, J_{HH} = 3.7 and 1.3 Hz), 7.66 (4H, dd, J_{HH} = 5.0 and 1.3 Hz), 7.09 (4H, dd, J_{HH} = 5.0 and 3.7 Hz).

[W_2(3-ThCO_2)$_4$]. The reaction was performed under similar conditions to those described for the preparation of [W_2(2-ThCO_2)$_4$] using 106 mg of [W_2(O_2C^tBu)$_4$] (0.137 mmol) and 70 mg of 3-ThCO_2H (0.549 mmol). A red solution formed immediately, from which a red solid precipitated after 5 min. The solution was allowed to stir for 1 day at room temperature. A red solid (104 mg, 86.5 % yield) was isolated by filtration and washed with small amounts of toluene and then hexane before being dried in vacuo. The product was virtually insoluble in THF.

Microanalysis found: C 25.56, H 1.72%. $C_{20}H_{12}O_8S_4W_2$ requires: C 27.41, H 1.38%.

[{(^{t}BuCO_2)$_3$Mo$_2$}$_2${2,5-Th(CO_2)$_2$}]. The reaction was carried out under similar conditions outlined for the tungsten analogue using 500 mg of [Mo_2(O_2C^tBu)$_4$] (0.838 mmol) and 72 mg of 2,5-Th(CO_2H)$_2$ (0.418 mmol). A red solid (435 mg, 90% yield) was isolated by filtration.

Microanalysis found: C 37.22; H 4.83%. $C_{36}H_{56}O_{16}SMo_4$ requires: C 37.26, H 4.86%. NMR (THF-d_8): δ_H (400 MHz) 7.29 (s, 2H, 2,5-C$_4H_2$S(CO_2)$_2$), 1.43 (s, 18H, $O_2CC(CH_3)_3$), 1.42 (s, 36H, $O_2CC(CH_3)_3$). MALDI-MS: 1162 (100%, M^+), 596 (10%, [Mo_2(O_2C^tBu)$_4$]$^+$).

[{(^{t}BuCO_2)$_3$W$_2$}$_2${2,5-Th(CO_2)$_2$}]. To a clear yellow solution of [W_2(O_2C^tBu)$_4$] (600 mg, 0.777 mmol) in toluene (ca. 20 cm^3) was added 2,5-Th(CO_2H)$_2$ (65 mg, 0.378 mmol) resulting in the almost instant formation of a deep blue solution. The reaction was stirred at room temperature for 5−10 days during which time a deep blue solid formed. This solid (545 mg, 95% yield) was collected by filtration and dried in vacuo after washing several times with small amounts of toluene and then hexanes.

Microanalysis found: C 27.05; H 3.89%. $C_{36}H_{56}O_{16}SW_4$ requires: C 28.59, H 3.73%. NMR (THF-d_8): δ_H (250 MHz) 7.28 (s, 2H, 2,5-C$_4H_2$S(CO_2)$_2$), 1.40 (s, 18H, $O_2CC(CH_3)_3$), 1.36 (s, 36H, $O_2CC(CH_3)_3$).

Attempted Preparation of [W_2(2,2′-BThCO_2)$_4$]. The reaction was performed under similar conditions to those described for the preparation of [W_2(2-ThCO_2)$_4$] using 500 mg of [W_2(O_2C^tBu)$_4$] (0.65 mmol) and 544 mg of 2,2′-BThCO_2H (2.59 mmol). The color changed immediately to a deep blue, and this solution was then stirred for 3 days at room temperature. A deep blue solid (699 mg) was isolated by filtration and then washed with toluene and then hexanes before being dried in vacuo. The desired product could not be isolated cleanly, and the ^{1}H NMR spectrum of the products showed residual 2,2′-BThCO_2H.

Attempted Preparation of [Mo_2(2,2″-TThCO_2)$_4$]. The reaction was performed under similar conditions to those described for the preparation of [Mo_2(2-ThCO_2)$_4$] using 0.41 g of [Mo(CO)$_6$] (1.56 mmol) and 1.0 g of 2,2″-TThCO_2H (3.42 mmol). A red solid was isolated from cooling the now red solution to room temperature. The isolated solid (1.2 g) was washed twice with hexanes (ca. 10 cm^3) and then dried in vacuo for 4 h. The product was only sparingly soluble in THF, and a satisfactory elemental analysis could not be obtained due to unidentified impurities.

Attempted Preparation of [W_2(2,2″-TThCO_2)$_4$]. The reaction was performed under similar conditions to those described for the preparation of [W_2(2-ThCO_2)$_4$] using 200 mg of [W_2(O_2C^tBu)$_4$] (0.26 mmol) and 303 mg of 2,2″-TThCO_2H (1.04 mmol). The color changed immediately to a deep blue, and this solution was then stirred for 3 days at room temperature. A deep blue solid was isolated by filtration and then washed with toluene and then hexanes before being dried in vacuo. The product was only sparingly soluble in THF, and a satisfactory elemental analysis could not be obtained.

Attempted Preparation of [{(^{t}BuCO_2)$_3$Mo$_2$}$_2${2,5′-BTh(CO_2)$_2$}]. Reaction conditions were the same as outlined for the preparation of [{W_2(O_2C^tBu)$_4$]$_3$}$_2${2,5-Th(CO_2)$_2$}] using 500 mg of [Mo_2(O_2C^t-Bu)$_4$] (0.838 mmol) and 107 mg of 2,5′-BTh(CO_2H)$_2$ (0.421 mmol). The compounds were stirred in toluene (20 mL) for 3 days. A red solid was isolated by filtration (365 mg) and washed with toluene before being dried in vacuo. A satisfactory microanlysis could not be obtained, and the ^{1}H NMR spectrum indicated unreacted starting material present among the products.

Attempted Preparation of [{(^{t}BuCO_2)$_3$W$_2$}$_2${2,5′-BTh(CO_2)$_2$}]. Reaction conditions were the same as outlined for the preparation of [{W_2(O_2C^tBu)$_4$]$_3$}$_2${2,5-Th(CO_2)$_2$}] using 412 mg of [W_2(O_2C^t-Bu)$_4$] (0.534 mmol) and 69 mg of 2,5′-BTh(CO_2H)$_2$ (0.267 mmol). During the 7 days of stirring, the solution changed from yellow to green to finally blue from which a blue solid precipitated from solution. This blue solid was filtered via a frit and washed several times with toluene then hexanes. A satisfactory microanalysis could not be obtained.

Attempted Preparation of [{(^{t}BuCO_2)$_3$M$_2$}$_2${2,5″-TTh(CO_2)$_2$}] (M = Mo, W). Reaction conditions were the same as outlined for the preparation of [{W_2(O_2C^tBu)$_4$]$_3$}$_2${2,5-Th(CO_2)$_2$}] using 2 equiv of [M_2(O_2C^tBu)$_4$] (500 mg) and 1 equiv of 2,5″-TTh(CO_2H)$_2$. The solution changed color slightly in both cases from yellow to mauve and green for molybdenum and tungsten, respectively. No formation of the bridged complex was detected after stirring for at least two weeks at room temperature by MALDI (M= Mo).

Attempted Preparation of [Mo_2(O_2CC(H)=C(H)-2-Th)$_4$]. [Mo(CO)$_6$] (2.00 g, 7.58 mmol) and 3-(2-thienyl)acrylic acid (2.37 g, 15.34 mmol) were dissolved in a mixture of 1,2-dichlorobenzene (ca. 100 cm^3) and THF (ca. 10 cm^3) in a Schlenk flask fitted with a reflux condenser. The solution was then heated to ca. 140 °C for 16 h during which time a red solution formed. After allowing the solution to cool slowly to room temperature, a red solid precipitated and was collected on a frit via filtration. The mother liquor was then layered with *n*-pentanes (ca. 100 cm^3) from which a red solid was collected by filtration via a frit. The solid (2.19 g) was washed twice with hexanes (ca. 40 cm^3) and then dried in vacuo for 4 h. A satisfactory microanalysis could not be obtained, and the ^{1}H NMR spectrum of the solid indicates a number of different products, presumably due to polymerization of the acrylic acid moiety.

Attempted Preparation of $[W_2(O_2CC(H)=C(H)\text{-}2\text{-}Th)_4]$. $[W_2(O_2C^tBu)_4]$ (460 mg, 0.596 mmol) was dissolved in toluene (ca. 10 cm^3) in a Schlenk flask, and to this clear yellow solution was added 3-(2-thienyl)acrylic acid (367 mg, 2.38 mmol). The color changed immediately to a deep blue, and this solution was then stirred for 3 h at room temperature during which a blue solid precipitated. This deep blue solid (540 mg, 93% yield) was filtered and then washed with toluene and then hexanes before being dried in vacuo. A satisfactory microanalysis could not be obtained.

Molecular and Electronic Structure Calculations. Molecular and electronic structure determinations on the models $[\{M_2(O_2CH)_3\}_2\{2,5\text{-}Th(CO_2)_2\}]$ (M = Mo, W) were performed with density functional theory (DFT) using the Gaussian 98[23] program, employing the B3LYP[24−26] functional in conjunction with the 6-31G* basis set for H, C, and O,[27] the 6-31+G(2d) basis set for S, and the SDD energy consistent pseudopotentials for Mo and W.[28] All geometries were fully optimized at the above levels using the default optimization criteria of the program. Orbital analyses were completed with GaussView.[29]

X-ray Crystallography. The data collection crystal for $Mo_2(O_2C\text{-}2\text{-}Th)_4\cdot 2THF$ was a red, multifaceted chunk. Examination of the diffraction pattern on a Nonius Kappa CCD diffractometer indicated a monoclinic crystal system. All work was done at 150 K using an Oxford Cryosystems Cryostream Cooler. The data collection strategy was set up to measure a quadrant of reciprocal space with a redundancy factor of 4. A combination of φ and ω scans with a frame width of 1.0° was used. Data integration was done with Denzo.[30] Scaling and merging of the data were done with Scalepack.[30]

The teXsan[31] package indicated the space group to be $P2_1/n$ on the basis of the systematic absences. The structure was solved by the Patterson method in SHELXS-86.[32] The Mo complex sits on an inversion center and has two THF molecules associated with it on each end. Full-matrix least-squares refinement based on F^2 was performed in SHELXL-93.[33] Each thienyl group is disordered by a 180° rotation about the C−COO bond. This is modeled by assuming that the following pairs of atoms occupy the same site: S(1) and C(3A), C(3) and S(1A), S(2) and C(8A), C(8) and S(2A). The occupancy factor for S(1) refined to 0.578(3), and the occupancy factor for C(3) was restrained to be equal to this value, since these two atoms belong to the same orientation of this ring. The other occupation for this ring [with S(1A) and C(3A)] has an occupancy factor of 0.422(3). For the other thienyl ring, the occupancy factor for one orientation is 0.898(3), with the other orientation at 0.102(3). The other atoms in the thienyl rings are assumed to be exactly overlapped in the two orientations of each ring, and so, their occupancy factors are 1.0. The hydrogen atoms were included in the model at calculated positions using a riding model with $U(H) = 1.2 \times U_{eq}$(bonded C atom). Experimental data relating to the structure determination are displayed in Table 1.

Table 1. Crystallographic Details for $Mo_2(O_2C\text{-}2\text{-}Th)_4\cdot 2THF$

empirical formula	$C_{28}H_{28}Mo_2O_{10}S_4$
fw	844.62
T (K)	150(2)
wavelength (Å)	0.71073
cryst syst	monoclinic
space group	$P2_1/n$
unit cell dimensions	
a (Å)	10.190(1)
b (Å)	9.943(1)
c (Å)	15.699(2)
β (deg)	91.636(1)
V (Å^3)	1589.9(3)
Z	2
D_{calc} (Mg m^{-3})	1.764
abs coeff (mm^{-1})	1.106
F(000)	848
cryst size (mm^3)	0.12 × 0.15 × 0.15
θ range for data collection (deg)	2.35−27.47
index ranges	$-13 \le h \le 13$ $-12 \le k \le 12$ $-20 \le l \le 20$
reflns collected	31328
indep reflns	3638 [$R_{int} = 0.027$]
refinement method	full-matrix least-squares on F^2
data/restraints/parameters	3638/0/201
GOF on F^2	1.085
final R indices [$I > 2\sigma(I)$]	$R_1 = 0.0237$, $wR_2 = 0.0584$
R indices (all data)	$R_1 = 0.0271$, $wR_2 = 0.0600$
largest difference peak and hole (e/Å^3)	0.640 and −0.469

Results and Discussion

Syntheses. The reactions between $[M_2(O_2C^tBu)_4]$ (M = Mo, W) compounds and thienyl carboxylic acids, 2-$ThCO_2H$ or 3-$ThCO_2H$ (see Scheme 2), in toluene proceed with the formation of a precipitate, and with an immediate color change from the yellow of the parent pivalate to the product color (see Experimental Section) as thienyl carboxylates are introduced to the metal center. When 1 equivalent of the thienyl dicarboxylic acid is added to $[M_2(O_2C^tBu)_4]$, the resulting solids appear to be a mixture of the compounds

Scheme 2

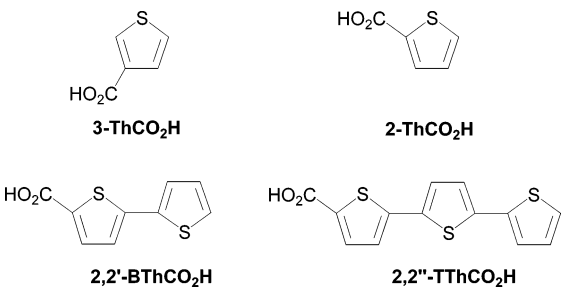

(23) Frisch, M. J.; Trucks, G. W.; Schlegel, H. B.; Scuseria, G. E.; Robb, M. A.; Cheeseman, J. R.; Zakrzewski, V. G.; Montgomery, J. A., Jr.; Stratmann, R. E.; Burant, J. C.; Dapprich, S.; Millam, J. M.; Daniels, A. D.; Kudin, K. N.; Strain, M. C.; Farkas, O.; Tomasi, J.; Barone, V.; Cossi, M.; Cammi, R.; Mennucci, B.; Pomelli, C.; Adamo, C.; Clifford, S.; Ochterski, J.; Petersson, G. A.; Ayala, P. Y.; Cui, Q.; Morokuma, K.; Malick, D. K.; Rabuck, A. D.; Raghavachari, K.; Foresman, J. B.; Cioslowski, J.; Ortiz, J. V.; Stefanov, B. B.; Liu, G.; Liashenko, A.; Piskorz, P.; Komaromi, I.; Gomperts, R.; Martin, R. L.; Fox, D. J.; Keith, T.; Al-Laham, M. A.; Peng, C. Y.; Nanayakkara, A.; Gonzalez, C.; Challacombe, M.; Gill, P. M. W.; Johnson, B. G.; Chen, W.; Wong, M. W.; Andres, J. L.; Head-Gordon, M.; Replogle, E. S.; Pople, J. A. *Gaussian 98*; Gaussian, Inc.: Pittsburgh, PA, 1998.
(24) Becke, A. D. *Phys. Rev. A: At., Mol., Opt. Phys.*. **1988**, *38*, 3098.
(25) Becke, A. D. *J. Chem. Phys.* **1993**, *98*, 5648.
(26) Lee, C.; Yang, W.; Parr, R. G. *Phys. Rev. B: Condens. Matter Mater. Phys.* **1988**, *37*, 785.
(27) Hehre, W. J.; Radom, L.; Schleyer, P. v. R.; Pople, J. A. *Ab initio Molecular Orbital Theory*; John Wiley & Sons: New York, 1986.
(28) Andrae, D.; Haeussermann, U.; Dolg, M.; Stoll, H.; Preuss, H. *Theor. Chim. Acta* **1990**, *77*, 123.
(29) Gaussian Inc.: Pittsburgh, PA, 1998.
(30) Otwinowski, Z.; Minor, W. *Macromolecular Crystallography, part A*; Carter, C. W., Jr., Sweet, R. M., Eds.; Methods in Enzymology, Vol. 276; Academic Press: New York, 1997; pp 307−326.
(31) 1.7-2 ed.; Molecular Structure Corporation: The Woodlands, TX, 1995.
(32) Sheldrick, G. M. *Acta Crystallog., Sect. A* **1990**, *46*, 467.
(33) Sheldrick, G. M. *SHELXL-93*; Universität Göttingen: Göttingen, Germany, 1993.

Scheme 3

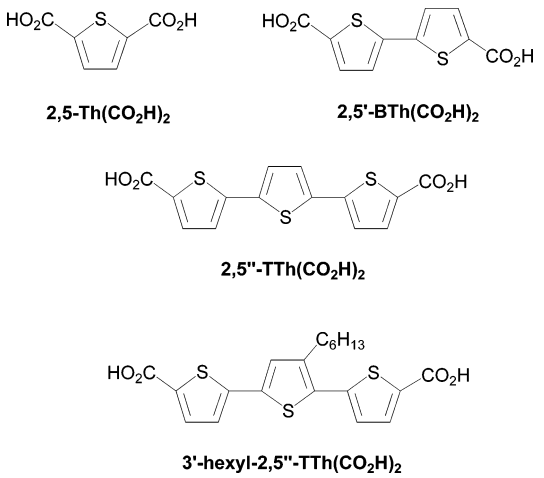

$[M_2(O_2C^tBu)_{4-x}(O_2CTh)_x]$ ($x = 0 \rightarrow 4$). With 4 equivalents of the thienyl carboxylic acid, the pivalate ligands can be successively replaced. The homoleptic compounds $[M_2(O_2CTh)_4]$ are difficult to obtain in an analytically pure form by this procedure, and some pivalate ligands bound to the M_2 center can be seen in both the MALDI mass spectrum and in the ^{1}H NMR spectra of the products. In the case of molybdenum, a more convenient route to introducing the thienyl carboxylate to the Mo_2^{4+} center involves refluxing the thienyl carboxylic acid in the presence of $[Mo(CO)_6]$ dissolved in a 1,2-dichlorobenzene and THF mixture.

A similar procedure was employed in the synthesis of the α,α′-linked bithienyl (2,2′-$BThCO_2H$) and terthienyl carboxylate (2,2′′-$TTThCO_2H$) derivates. With increasing numbers of thienyl units, the M_2^{4+} containing compounds became less soluble and less easy to purify by recrystallization as the bi- and ter-thienyl-2-carboxylic acids were themselves only sparingly soluble. There is, however, little doubt that tetra substitution at the M_2^{4+} center was achieved, and all the Mo_2^{4+}-containing compounds showed parent molecular ions with the characteristic Mo_2-isotopic pattern in the MALDI-MS. The Mo_2-containing complexes appear to be air-stable in the solid state for days, whereas the analogous tungsten complexes decompose within minutes.

The reactions between 2 equivalents of $[M_2(O_2C^tBu)_4]$ (M = Mo, W) and 1 equivalent of thiophene-2,5-dicarboxylic acid led to the precipitation of the microcrystalline powders $[\{(Bu^tCO_2)_3M_2\}_2(\mu\text{-}2,5\text{-}Th(CO_2)_2)]$. These compounds were not appreciably soluble in toluene but were soluble in tetrahydrofuran. Related reactions involving α,α′-linked bithienyl and terthienyl 2,5′-dicarboxylic acids (see Scheme 3) and $[M_2(O_2C^tBu)_4]$ (M = Mo, W) were also examined and precipitates obtained from toluene contained the corresponding M_4 dicarboxylates contaminated with some of the free dicarboxylic acids which were, themselves, not very soluble in toluene. In the case of the bithienyldicarboxylates, the spectroscopic data and electrochemical data reported later leave little doubt that the desired compounds were obtained, if not in an entirely pure form in this reaction sequence.

In the reactions involving $[M_2(O_2C^tBu)_4]$ and 3-(2-thienyl)-acrylic acid (in excess in toluene), the compound $[M_2(O_2CCH{=}CH\text{-}2\text{-}Th)_4]$ was formed and isolated, but it was not completely free from the partially substituted compounds of the form $[M_2(O_2C^tBu)_{4-x}(O_2CCH{=}CH\text{-}2\text{-}Th)_x]$ ($x = 1-3$). Attempts to prepare $[Mo_2(O_2CCH{=}CH\text{-}2\text{-}Th)_4]$ from the reaction between $[Mo(CO)_6]$ and the free acid did not lead to a pure compound. Prolonged heating resulted in the formation, in the ^{1}H NMR spectrum, of new aliphatic resonances that presumably arise from the polymerization of the acrylate groups.

Whereas satisfactory elemental analyses were obtained for selected molybdenum complexes, the analogous tungsten complexes were low in carbon by ca. 1.5%. A similar finding was noted earlier for related tungsten compounds.[34] Although the ^{1}H NMR spectra of these compounds are consistent with expectations, we cannot discount impurities arising from incomplete pivalate replacement, the presence of trace amounts of free carboxylic acids, or trace decomposition due to their air-sensitivity. Molecular ions with the characteristic isotopic patterns for the presence of two or four metal ions were seen in the MALDI-MS for molybdenum complexes and for some tungsten complexes. Due to the air-sensitive nature of the tungsten complexes, few were submitted for MS analysis.

^{1}H NMR data for some of these new compounds are given in the Experimental Section and are as expected for the formulation given. However, as the length of the thiophene chain increases, the solubility of the complexes decreases, and in some instances, it was not sufficient to record NMR spectra. In all cases, the compounds appear to be diamagnetic.

The radical cations of the 2,5-thienyl dicarboxylate bridge complexes were prepared by treatment of the neutral complex with 1 equivalent of $[Cp_2Fe]^+[PF_6]^-$ in a THF/CH_2Cl_2 mixture. The freshly prepared samples were examined by EPR spectroscopy. No attempt to isolate the cationic complexes was made, and crystalline solids have thus far not been successfully isolated.[35]

Crystal and Molecular Structure of $Mo_2(O_2C\text{-}2\text{-}Th)_4\cdot 2THF$. Crystals of $Mo_2(O_2C\text{-}2\text{-}Th)_4\cdot 2THF$ were obtained by crystallization from a THF solution, and in the space group $P2_1/n$ the molecule lies on a crystallographically imposed center of inversion. A view of the molecule is shown in Figure 1, and pertinent bond distances and angles are given in the figure caption. The molecule is quite unexceptional with respect to $Mo_2(O_2CR)_4$ compounds in terms of M−M and M−O distances but is useful with respect to showing the near coplanarity of the thienyl ring and the CO_2 carboxylate groups. The C3−C2−C1−O2 and C8−C7−C6−O3 dihedral angles of 3.9(4)° and 9.2(3)°, respectively, favor electronic communication between the M_2 δ orbitals and the thienyl π-system. In the molecular structure shown in Figure 1, only one position of the otherwise disordered thienyl rings is shown. The disorder involves a 180° rotation of the ring about the carboxylate carbon to thienyl carbon

(34) Byrnes, M. J.; Chisholm, M. H.; Dye, D. F.; Hadad, C. M.; Pate, B. D.; Wilson, P. J.; Zaleski, J. M. *J. Chem Soc., Dalton Trans.* **2004**, 523.

(35) Chisholm, M. H.; Pate, B. D. Unpublished results.

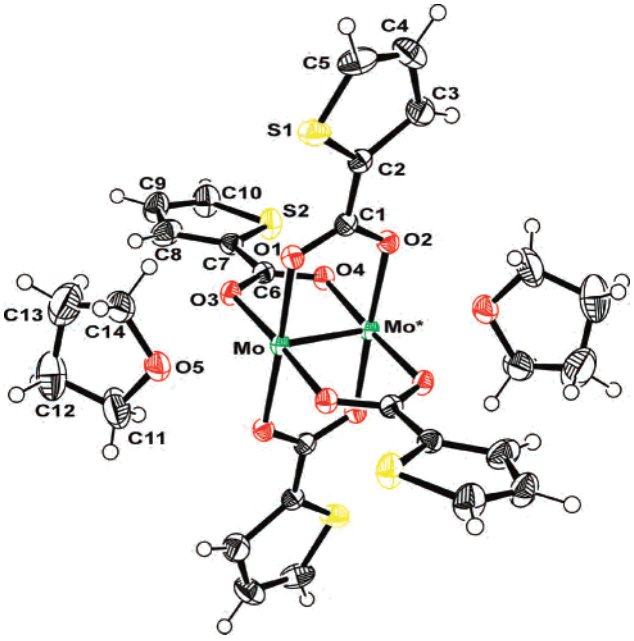

Figure 1. Molecular structure of $Mo_2(O_2C\text{-}2\text{-}Th)_4 \cdot 2THF$ with the anisotropic displacement parameters drawn at the 50% probability level. Only the major orientation of the disordered thienyl rings is shown, and one-half of the molecule is symmetry generated using a center of inversion. Selected bond lengths: Mo−Mo* = 2.1082(3) Å, Mo−$O_{carboxylate}$ (average) = 2.11 Å, Mo−O5 = 2.587(2) Å.

bond which precludes a detailed discussion of bond distances within the five-membered ring that might otherwise have provided evidence for Mo_2 δ to ligand π^* back-bonding to the thienyl LUMO shown in drawing A, vide infra. Inspection of the packing in the solid state structure reveals the onset of thienyl ring−ring interactions between molecules, shown in Figure 2. We anticipate that this will become more important for bi- and ter-thienyl derivatives.

UV−Vis Spectra. The new compounds have intense absorptions in the visible region of the spectrum as a result of the fully allowed metal-to-ligand charge transfer transition: M_2 δ to Th π^*. A comparison of the spectra for the molybdenum complexes is shown in Figure 3. MO calculations on the free carboxylates employing density functional theory (B3LYP)[24−26] and the Gaussian 98 suite of programs[23] are useful in terms of correlating the trends. First, substitution of the carboxylate group at the 2-position (α) relative to the 3-position (β) in the thienyl ring is more effective in promoting electronic coupling, and the LUMO of the 2-$ThCO_2^-$ ligand is the lower in energy. It takes the form shown diagrammatically in drawing A. This orbital is C−O π^* and C−C π bonding. Placing an electron in this orbital will favor coplanarity of the CO_2 and thienyl ring.

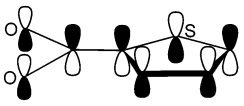

A

Inspection of the spectra of the 2-$ThCO_2$ and 3-$ThCO_2$ molybdenum complexes reveals that the electronic transition assignable to M_2 δ to L π^* occurs at lower energy and with greater intensity for the former, consistent with the expectations based on MO theory as just described.

In changing the carboxylate from thienyl (Th) to bithienyl (BTh) to terthienyl (TTh) carboxylates, the HOMO rises in energy, and the LUMO descends. The LUMO of 2,2″-$TThCO_2^-$ takes the form of the orbital interaction depicted in drawing B. For any polythiophene-2-CO_2^- ligand, the LUMO will be C−O π^* and have C−C π interactions akin to those shown in drawing B.

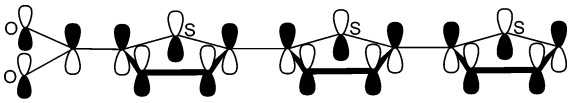

B

Inspection of the electronic spectra shown in Figure 3 reveals the red shift that occurs in the lowest allowed transition as each thienyl unit is added to the chain. Also, with increasing number of thienyl rings, we observe that the ligand π to π^* electronic transition moves to lower energy.

The spectra of the tungsten containing complexes are shown in Figure 4. The intense and broad electronic transitions assignable to W_2 δ to L π^* are notably red-shifted compared to the respective molybdenum spectrum. With each additional thienyl ring, this transition is further red-shifted, and the compound $[W_2(O_2C\text{-}2,2''\text{-}TTh)_4]$ has its maximum intensity well into the near-IR. The ligand-based π to π^* transitions are very similar in energy to those seen for the molybdenum analogues. The relative intensities of the W_2 δ to thienyl π^* transitions are notably greater than those for their molybdenum analogues. This, together with the notable red-shift observed when M = W (relative to Mo), is understandable on the basis of the higher energy of the W_2 δ orbitals (by ca. + 0.5 eV)[10] and the greater degree of overlap, W_2 δ with L π^*.

In the case of $[W_2(O_2C\text{-}2\text{-}Th)_4]$, there is clear evidence of a vibronic progression associated with the O_2C-2-Th unit. Upon lowering the temperature of a sample in 2-MeTHF, this progression becomes more pronounced, and the onset of the (0,0) transition becomes sharper and moves to longer wavelength. The introduction of a carbon−carbon double bond between the carboxylate and the thienyl ring generates the 3-(2-thienyl)acrylate ligand, $O_2C(CH{=}CH)$-2-Th, and extends the degree of conjugation and lowers the LUMO, resulting in the movement of the (0,0) transition to lower energy.

The breadth of the M_2 δ to L π^* transition probably reflects the varying dihedral angles between the O_2C plane and the plane of the thienyl ring. Also, upon each addition of a thienyl unit, the relative orientation of one ring with respect to its neighbors is another variable that will cause a broadening of the absorption band and a loss of the vibronic features. Upon lowering the temperature, the Boltzmann distribution of rotamers present in a solution or glass will more closely resemble the minimum energy structure that maximizes π-conjugation. Consequently, we observe a red-shift and an increase in the resolution of vibronic features upon cooling samples in 2-MeTHF.

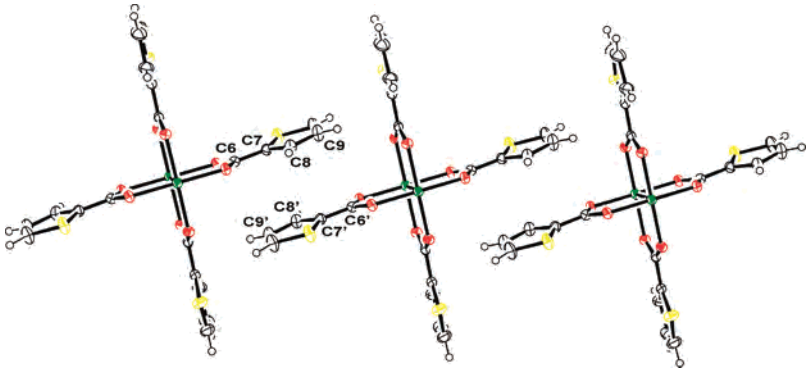

Figure 2. Molecular packing diagram for $Mo_2(O_2C\text{-}2\text{-}Th)_4 \cdot 2THF$ showing thienyl ring−ring interactions. Selected bond lengths: C6−C9′ = 3.477(3) Å, C7−C8′ = 3.398(3) Å.

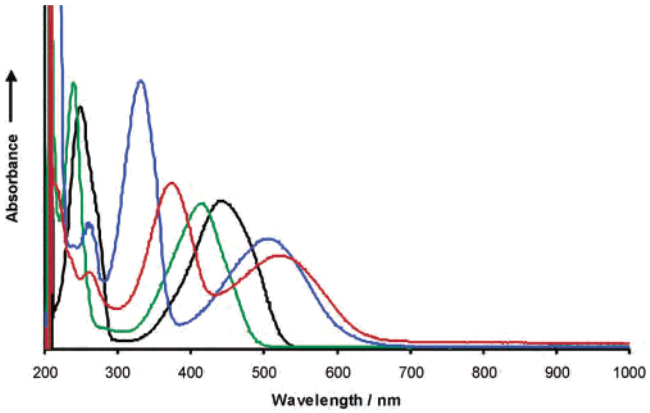

Figure 3. UV−vis spectra of $[Mo_2(3\text{-}ThCO_2)_4]$ (green), $[Mo_2(2\text{-}ThCO_2)_4]$ (black), $[Mo_2(2,2'\text{-}BThCO_2)_4]$ (blue), and $[Mo_2(2,2''\text{-}TThCO_2)_4]$ (red) in THF at room temperature.

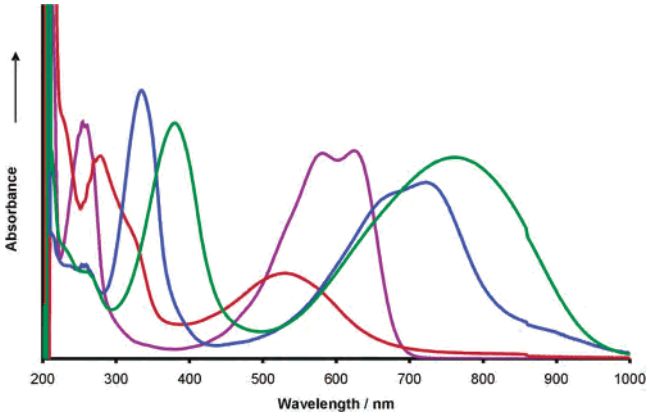

Figure 4. UV−vis spectra of $[W_2(3\text{-}ThCO_2)_4]$ (red), $[W_2(2\text{-}ThCO_2)_4]$ (purple), $[W_2(2,2'\text{-}BThCO_2)_4]$ (blue), and $[W_2(2,2''\text{-}TThCO_2)_4]$ (green) in THF at room temperature.

A summary of the spectral data for the compounds reported herein is given in Table 2, and a simplified interpretation of the spectra is presented in the schematic MO diagram shown in Figure 5.

Bridged Complexes. The electronic absorption spectra of the 2,5-thienyl dicarboxylate bridged compounds are compared in Figure 6. We again see the lower energy of the M_2 δ-to-bridge π^* transition for tungsten than molybdenum, with evidence of a vibronic progression for M = W. This absorption is also much more intense for the former. At higher energy, there is the M_2 δ to CO_2 π^* transition associated with the pivalates and, at even higher energy, the bridge π to π^* absorption. These spectra in some way resemble the perfluoroterephthalate complexes $[\{(^tBuCO_2)_3M_2\}_2(\mu\text{-}O_2CC_6F_4CO_2)]$ discussed in some detail in a recent publication.[14]

At low temperatures, the spectra red-shift and sharpen, and the vibronic progression becomes more clearly resolved, as shown in Figure 7 for $[\{(^tBuCO_2)_3W_2\}_2\{\mu\text{-}2,5\text{-}Th(CO_2)_2\}]$. A frontier MO diagram for these complexes is given in Figure 8, and the spectral data are listed alongside that of the homoleptic compounds in Table 2.

Table 2. Electronic Absorption Data for the Various Carboxylate and Dicarboxylate Complexes of Dimolybdenum and Ditungsten at 298 K in THF

compound	λ_{max} (nm) in THF	ϵ (M^{-1} cm^{-1}) in THF
$[Mo_2(O_2C\text{-}2\text{-}Th)_4]$	441	18 850
	248	30 900
$[W_2(O_2C\text{-}2\text{-}Th)_4]$	624	20 000
	583	20 000
	256	31 200
$[Mo_2(O_2C\text{-}3\text{-}Th)_4]$	415	11 850
	239	21 750
$[W_2(O_2C\text{-}3\text{-}Th)_4]$	525	2400
	328	3550
	278	5700
	226	7000
$[Mo_2(O_2C\text{-}2\text{-}BTh)_4]$	507	21 750
	332	52 850
$[W_2(O_2C\text{-}2\text{-}BTh)_4]^a$	723	
	662	
	333	
$[Mo_2(O_2C\text{-}2\text{-}TTh)_4]^a$	521	
	373	
$[W_2(O_2C\text{-}2\text{-}TTh)_4]^a$	760	
	379	
$[\{(^tBuCO_2)_3Mo_2\}_2(\mu\text{-}2,5\text{-}Th(CO_2)_2)]$	515	16 000
	322	13 050
	277	26 600
$[\{(^tBuCO_2)_3W_2\}_2(\mu\text{-}2,5\text{-}Th(CO_2)_2)]$	797	35 900
	720	31 500
	640	16 100
	362	21 450
	282	11 100
$[\{(^tBuCO_2)_3Mo_2\}_2(\mu\text{-}1,4\text{-}C_6F_4(CO_2)_2)]^b$	470	10 500
	322 sh	11 900
	288	18 000
$[\{(^tBuCO_2)_3W_2\}_2(\mu\text{-}1,4\text{-}C_6F_4(CO_2)_2)]^b$	816	27 000
	354	17 300

[a] Due to sample impurities (see Experimental Section), the accurate concentration could not be determined; hence, there is no value for ϵ. [b] Taken from ref 11.

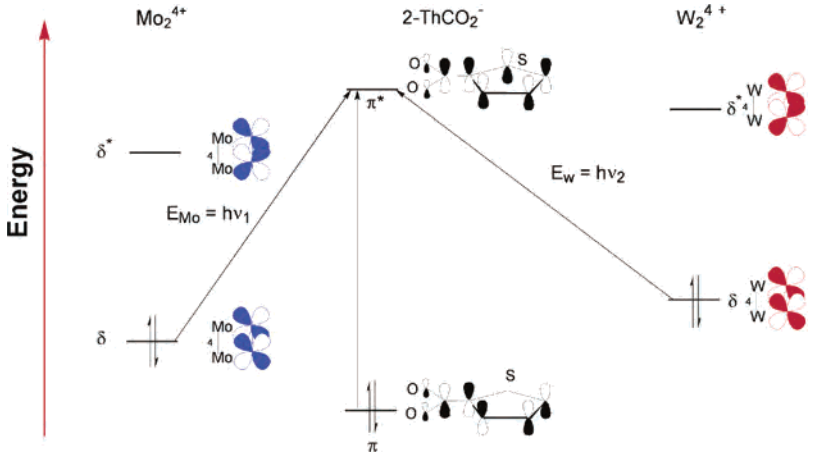

Figure 5. Schematic MO diagram for $M_2(2\text{-ThCO}_2)_4$ (M = Mo, W) compounds, highlighting the lower energy of the tungsten $\delta \rightarrow \pi^*$ transition over that of molybdenum.

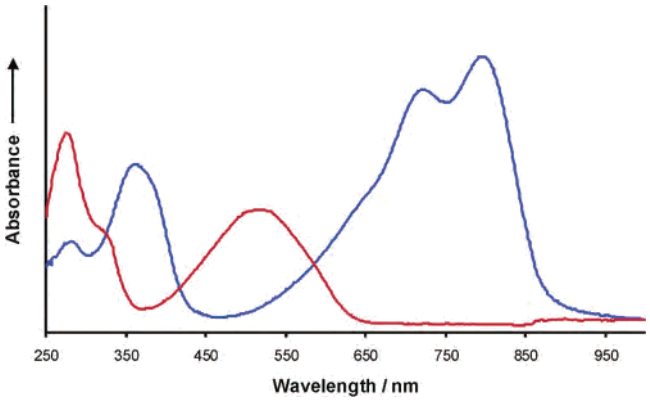

Figure 6. Electronic absorption spectra of $[\{(^t\text{BuCO}_2)_3\text{Mo}_2\}_2\{\mu\text{-2,5-Th}(\text{CO}_2)_2\}]$ (red) and $[\{(^t\text{BuCO}_2)_3\text{W}_2\}_2\{\mu\text{-2,5-Th}(\text{CO}_2)_2\}]$ (blue) in THF at room temperature.

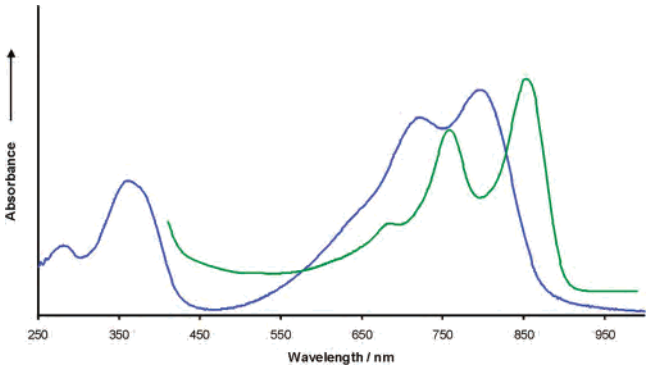

Figure 7. Electronic absorption spectra of $[\{(^t\text{BuCO}_2)_3\text{W}_2\}_2\{\mu\text{-2,5-Th}(\text{CO}_2)_2\}]$ at 298 K in THF (blue) and at 12 K (green) in 2-MeTHF.

Electronic Structure Calculations. Calculations employing density functional theory were carried out on the model compounds $[\{(\text{HCO}_2)_3\text{M}_2\}_2\{\mu\text{-2,5-Th}(\text{CO}_2)_2\}]$. The minimum energy structures were found having virtual C_{2v} symmetry and a near planar $\text{M}_2\{\mu\text{-O}_2\text{C}(\text{C}_4\text{H}_2\text{S})\text{CO}_2\}\text{M}_2$ unit. This allows for maximum M_2 δ-to-bridge π conjugation and is directly analogous to that described in detail for oxalate and perfluoroterephthalate bridged compounds.[13,14] The two M_2 δ combinations, the in-phase and out-of-phase, are significantly separated in energy as a result of interactions with the bridge. The HOMO is the out-of-phase combination and lies ca. 0.2 eV (M = Mo) and 0.3 eV (M = W) higher than the in-phase combination which is stabilized by M_2 δ-to-bridge π^* bonding. The HOMO of the W_4-containing complex is 0.5 eV higher in energy than its counterpart in the Mo_4-containing complex. The LUMO is, in both cases, the bridge-centered π^* MO that is involved in stabilizing the M_2 δ combination that forms the HOMO − 1. The calculations on these model compounds place the HOMO−LUMO gap at 2.8 eV (M = Mo) and 2.3 eV (M = W). These frontier orbitals are depicted in Figure 9 for the molybdenum complex.

On the basis of the orbital energies that are calculated for the free thienyl carboxylic acids, we can reasonably estimate the electronic composition of the frontier orbitals of the bi- and ter-thienyl dicarboxylate bridged compounds. In all cases, the filled M_2 δ orbitals lie higher in energy than the HOMOs of the thienyl bridges, and the bridge π^* LUMO orbitals lie below the M_2 δ^* orbitals. We, therefore, expect that oxidation will always be metal-centered and reduction will be thienyl-based. With an increasing number of thienyl units, the HOMO of the bridge rises in energy such that it lies between the Mo_2 π and the Mo_2 δ orbitals and, in the case of tungsten, lies between the W_2 σ and W_2 π orbitals.

Electrochemical Studies. The compounds $[\text{M}_2(\text{O}_2\text{C-2-Th})_4]$ in THF showed one reversible oxidation wave associated with the removal of a δ-electron in the $M_2^{4+/5+}$ cycle. The $[\{(^t\text{BuCO}_2)_3\text{M}_2\}_2\{\mu\text{-2,5-Th}(\text{CO}_2)_2\}]$ compounds showed two oxidation processes in the cyclic voltammograms, the first electrochemically reversible, the second only quasireversible. As has been noted before for these types of bridged dinuclear systems, the separation of these two oxidation processes, which is most accurately measured by differential pulsed voltammetry, is a measure of the electronic coupling of the two M_2 centers via the bridge.[11] This separation, $\Delta E_{1/2}$, is larger for the tungsten complex and comparable to that of the perfluoroterephthalate bridge complex.[14] With increasing distance between the M_2 centers, the $\Delta E_{1/2}$ value falls off and both bithienyl dicarboxylate bridged complexes may be considered to be valence-trapped as shown in Figure 10. The bridged compounds also show a quasireversible reduction wave, which we attribute to the reduction of the bridge.

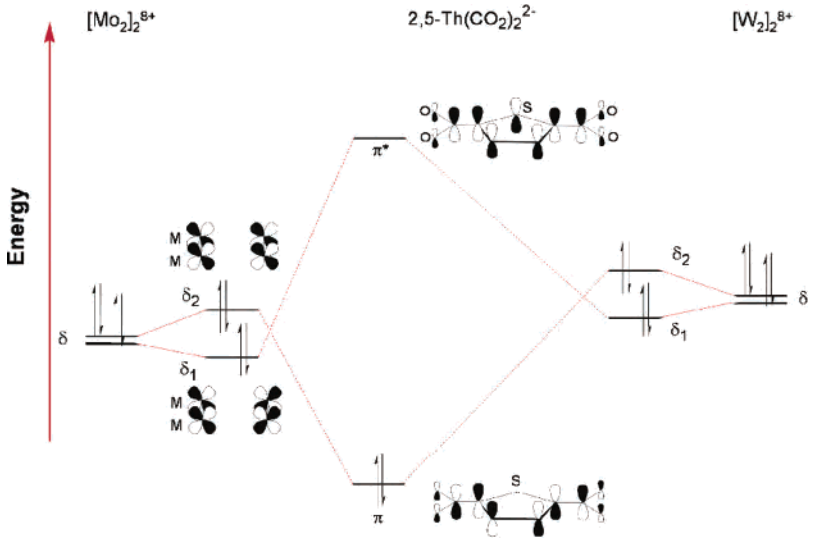

Figure 8. Schematic frontier MO diagram for $[(^tBuCO_2)_3M_2]_2(\mu\text{-}2,5\text{-}Th(CO_2)_2)$ (M = Mo, W) complexes.

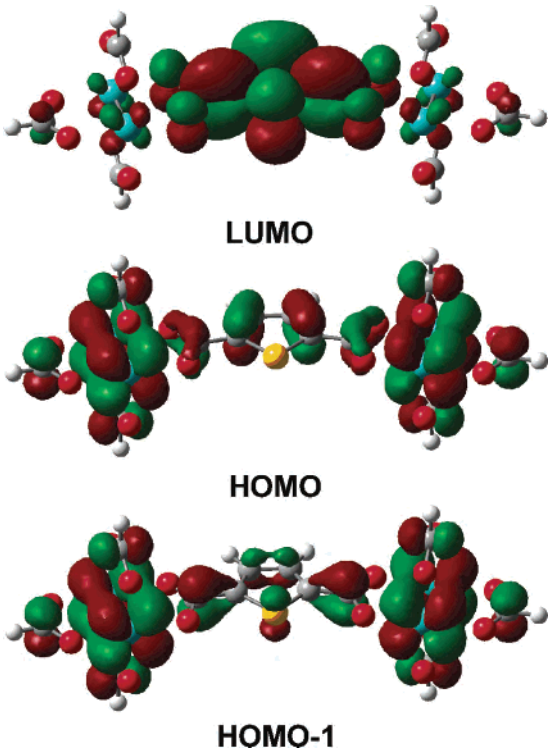

Figure 9. Molecular orbital plots of $[\{W_2(O_2CH)_3\}_2\{2,5\text{-}Th(CO_2)_2\}]$ in C_2 symmetry (0.02 isosurface contour): 6-31G* basis set for C, H, and O; 6-31G$^+$(2d) basis set for S; Stuttgart RSC basis for W.

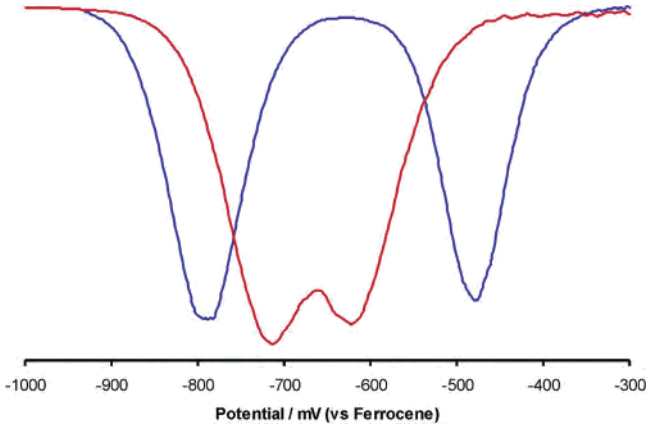

Figure 10. Differential pulse voltammetry (DPV) of $[\{(^tBuCO_2)_3W_2\}_2(\mu\text{-}2,5\text{-}Th(CO_2)_2)]$ (blue) and $[\{(^tBuCO_2)_3W_2\}_2(\mu\text{-}2,5\text{-}BTh(CO_2)_2)]$ (red) in 0.5M ^{n}Bu$_4$PF$_6$/THF showing the two oxidation processes relative to ferrocene. Scan rate is 5 mV s^{-1}.

Electrochemical data are presented in Table 3 for these and related complexes.

EPR Spectra. The metals molybdenum and tungsten have spin-active nuclei among their several naturally occurring isotopes. ^{95}Mo and ^{97}Mo have $I = {}^5/_2$, a very similar magnetic moment, and occur in a combined abundance of 28%. Consequently, a typical d^1-Mo-containing isotropic EPR spectrum consists of a central signal flanked by a hyperfine spectrum. When the odd electron is delocalized over more than one molybdenum center, the satellite spectrum changes to reflect the probability of the isotopic distribution, and the A_0 value, the hyperfine coupling constant, is reduced due to electron delocalization. The EPR spectrum of the radical cation $[\{(^tBuCO_2)_3Mo_2\}_2\{\mu\text{-}2,5\text{-}Th(CO_2)_2\}]^+$ in THF/CH_2Cl_2 at 298 K is shown in Figure 11. The spectrum consists of a central resonance, $g_0 = 1.943$, flanked by six lines due to coupling to one of the spin-active Mo nuclei (^{95}Mo or ^{97}Mo), $A_0 = 27.4$ G. Careful inspection of the satellite spectrum reveals resonances arising from molecules having two spin-active Mo nuclei. From the magnitude of the A_0 value and the relative intensities of the satellite spectrum, it is evident that the system is valence-trapped on the EPR timescale. That is to say that one Mo_2 center is +5 with a single δ electron and the other Mo_2 center remains Mo_2^{4+} with the δ^2 configuration. The spectrum very closely resembles that seen for the perfluoroterephthalate bridged compound $[\{(^tBuCO_2)_3Mo_2\}_2(\mu\text{-}O_2CC_6F_4CO_2)]^+[PF_6]^-$ which was valence trapped, $g_0 = 1.942$, $A_0 = 27.2$ G, and is quite different from that seen for the oxalate bridged compound $[\{(^tBuCO_2)_3Mo_2\}_2(\mu\text{-}O_2CCO_2)]^+[PF_6]^-$ which was delocalized, $g_0 = 1.937$, $A_0 = 14.8$ G.[15]

In the case of tungsten, just one isotope is spin active, namely ^{183}W, $I = {}^1/_2$, 14.5% natural abundance. The EPR spectrum of $[\{(^tBuCO_2)_3W_2\}_2\{\mu\text{-}2,5\text{-}Th(CO_2)_2\}]^+[PF_6]^-$ in

Table 3. Comparison of Electrochemical Oxidation Potentials[a] for Various Linked and Unlinked MM Quadruply Bonded Complexes with Pivalate Ligands in THF Referenced to $[Cp_2Fe]^{0/+}$

compd	$E_{1/2}{}^1$ [a] (V)	$E_{1/2}{}^2$ [a] (V)	$\Delta E_{1/2}$ (mV)
$[(^tBuCO_2)_3Mo_2\}_2(\mu\text{-}2,5\text{-}Th(CO_2)_2)]$	−0.04	0.07	110
$[\{(^tBuCO_2)_3W_2\}_2(\mu\text{-}2,5\text{-}Th(CO_2)_2)]$	−0.79	−0.48	310
$[\{(^tBuCO_2)_3Mo_2\}_2(\mu\text{-}2,5\text{-}BTh(CO_2)_2)]$[b]	−0.03		
$[\{(^tBuCO_2)_3W_2\}_2(\mu\text{-}2,5\text{-}BTh(CO_2)_2)]$	−0.72	−0.63	90
$[\{(^tBuCO_2)_3Mo_2\}_2(\mu\text{-}C_2O_4)]$[c]	−0.03	+0.25	280
$[\{(^tBuCO_2)_3W_2\}_2(\mu\text{-}C_2O_4)]$[c]	−1.26	−0.54	717
$[\{(^tBuCO_2)_3Mo_2\}_2(\mu\text{-}1,4\text{-}C_6F_4(CO_2)_2)]$[b,c]	+0.10		65
$[\{(^tBuCO_2)_3W_2\}_2(\mu\text{-}1,4\text{-}C_6F_4(CO_2)_2)]$[c]	−0.66	−0.37	285
$[\{(^tBuCO_2)_3W_2\}_2(\mu\text{-}1,8\text{-}An(CO_2)_2)]$[c]	−0.66	−0.51	156
$[\{(^tBuCO_2)_3W_2\}_2(\mu\text{-}1,1'\text{-}Fe(\eta^5\text{-}C_5H_4CO_2)_2)]$[c]	−0.81	−0.72	93
$[\{(^tBuCO_2)_3Mo_2\}_2(\mu\text{-}9,10\text{-}An(CO_2)_2)]$[d]	+0.04	+0.10	60
$[\{(^tBuCO_2)_3W_2\}_2(\mu\text{-}9,10\text{-}An(CO_2)_2)]$[d]	−0.62	−0.53	90
$[Mo_2(O_2C^tBu)_4]$[c]	−0.04		
$[W_2(O_2C^tBu)_4]$[c]	−0.70		
$[Mo_2(O_2C\text{-}2\text{-}Th)_4]$	−0.03		
$[W_2(O_2C\text{-}2\text{-}Th)_4]$	−0.67		
$[Mo_2(O_2C\text{-}2\text{-}BTh)_4]$	−0.03		
$[W_2(O_2C\text{-}2\text{-}BTh)_4]$	−0.61		
$[Mo_2(O_2C\text{-}2\text{-}TTh)_4]$	−0.04		
$[W_2(O_2C\text{-}2\text{-}TTh)_4]$	−0.66		

[a] $E_{1/2}{}^1$ and $E_{1/2}{}^2$ values correspond to $E_p{}^1$ and $E_p{}^2$, respectively. No attempt has been made to convert E_p to $E_{1/2}$ according to the methodology of Richardson and Taube.[36] [b] The potential represents the average $E_{1/2}$ for both redox couples involving the removal of one electron. [c] Taken from ref 11. [d] Taken from ref 34.

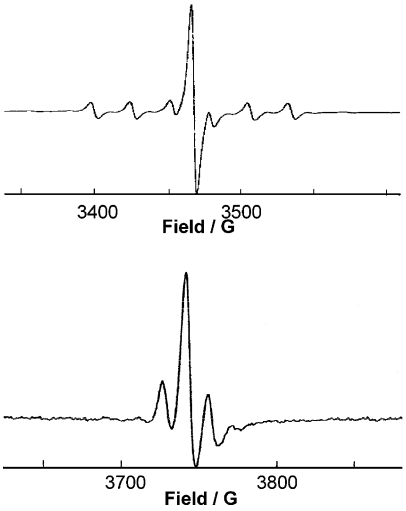

Figure 11. EPR spectra of radical cations $[\{^tBuCO_2)Mo_2\}_2(\mu\text{-}2,5\text{-}Th(CO_2)_2)]^+$ (top) at 298 K and $[\{^tBuCO_2)W_2\}_2(\mu\text{-}2,5\text{-}Th(CO_2)_2)]^+$ (bottom) at 210 K in a mixture of THF/CH_2Cl_2.

THF/CH_2Cl_2 at 210 K is also shown in Figure 11. From the magnitude of the satellite spectrum and the A_0 value, we can conclude that this spectrum arises from a single electron that is delocalized over all four tungsten centers: $g_0 = 1.832$, $A_0 = 29.7$ G. In the Robin and Day classification scheme,[37] this is a fully delocalized mixed valence complex on the EPR time-scale, 10^{-10} s^{-1}, class III. The greater delocalization for tungsten parallels what was seen previously for perfluoroterephthalate bridged complexes and supports the MO picture presented earlier on the basis of the calculations employing density functional theory.[38] The very low value of g_0 for the tungsten complex reflects the significance of spin−orbit coupling in this heavy metal system. The oxidation, in both cases, is metal centered and effectively delocalized in the case of the tungsten via W_2 δ-to-bridge π bonding.

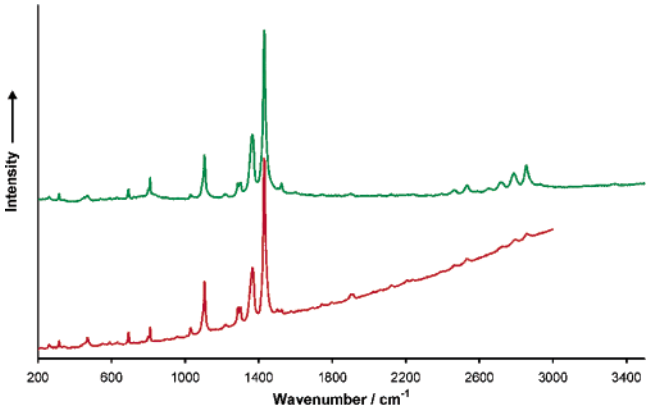

Figure 12. Raman spectrum of $[(^tBuCO_2)_3W_2]_2(\mu\text{-}2,5\text{-}Th(CO_2)_2)$ with laser excitation at 515 nm (green) and 633 nm (red).

Table 4. Comparison of the Wavenumber of the Experimental Resonance Raman Bands of $[\{(^tBuCO_2)_3W_2\}_2(\mu\text{-}2,5\text{-}Th(CO_2)_2)]$ with Those Calculated for $[\{(HCO_2)_3W_2\}_2(\mu\text{-}2,5\text{-}Th(CO_2)_2)]$ Together with the Band Assignments

exptl ν/cm^{-1}	calcd ν/cm^{-1}	assignment
316	337	W_4 symmetric stretch
472	486	W−O(bridge) symmetric stretch
693	698	W−O(bridge) and S−C symmetric stretching
810	819	bridge breathing
1106	1141	symmetric bridge C−C stretch
1293	1331	symmetric ring stretch
1308	1339	symmetric ring stretch
1368	1431	ring C−C and O_2C−C(ring) symmetric stretch
1431	1484	ring C−C and O_2C−C(ring) symmetric stretch

Resonance Raman Spectra. The intensely absorbing compounds in the visible region lend themselves to Raman studies in which the spectrum is obtained with various excitation lines. Excitation into the metal-to-ligand/bridge charge transfer band is expected to lead to resonance enhancement of vibrational bands that reflects a significant change in distance between the ground state and photoexcited state structures.[39] We have not as yet made a systematic study of this for this class of new compounds, but we have examined the 2,5-thienyl dicarboxylate bridged compounds and these clearly do show resonance Raman enhanced bands. The Raman spectra of the tungsten complex are shown in Figure 12 with excitation at two different frequencies. Both fall within the broad metal-to-bridge charge transfer band, and several bands show significant resonance enhancement. On the basis of the calculated Raman spectrum for the model compound $[\{(HCO_2)_3W_2\}_2\{\mu\text{-}2,5\text{-}Th(CO_2)_2\}]$, we offer the assignments shown in Table 4. The most enhanced bands are associated with symmetric vibrations of the bridging

(36) Richardson, D. E.; Taube, H. *Inorg. Chem.* **1981**, *20*, 1278.
(37) Robin, M. B.; Day, P. *Adv. Inorg. Radiochem.* **1967**, *10*, 247.
(38) Parr, R. G.; Yang, W. *Density Functional Theory of Atoms and Molecules*; Oxford University Press: Oxford, 1989.
(39) Clark, R. J. H.; Dines, T. J. *Angew. Chem., Int. Ed.* **1986**, *25*, 131.

thienyl dicarboxylate, and as is evident from the movie (see Supporting Information), the band at ca. 1480 cm^{-1} is associated with ν(CC) of the carboxylate carbon to ring carbon and 3,3′-carbons of the ring. This is consistent with placing an electron into the LUMO (described earlier) in the photoexcited state. It is also likely that it is this vibrational mode which gives rise to the vibronic structure in the electronic absorption spectrum, although the wavenumber of this mode is, as expected, more than it is in the Raman spectrum. The latter reflects the ground-state molecule, and the vibronic progression in the electronic spectrum is associated with the photoexcited state of the molecule which has an electron in the quinoidal-like LUMO depicted in drawing C (see also Figure 9).

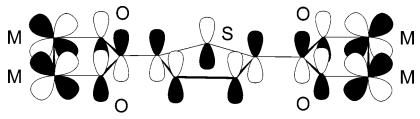

C

Concluding Remarks

The present work confirms our expectation that the carboxylate group is a good electronic linker between the M_2 quadruply bonded center and the thienyl unit and also highlights some of the practical difficulties of incorporating M_2 units into a polymer. The solubilities of the starting materials, intermediates, and products play a crucial role in obtaining analytically pure samples. The dicarboxylic acids and the intermediates produced by the replacement of one pivalate, $[(^tBuCO_2)_3M_2(O_2CXCO_2H)]$ (where X = bridge) need to be sufficiently soluble to allow for the second M_2 unit to form the bridged complex. At that point, precipitation from solution drives the reaction to the desired product. If the dicarboxylic acid and/or the monosubsituted intermediate are not sufficiently soluble, then the desired bridged complex will not form. If the bridged compound is soluble, then further substitution will occur yielding higher order oligomers.

Collectively, the compounds described here have chromophores that span the entire region of the visible spectrum and can be extended well into the near-IR. The intensity and breadth of these absorptions, especially those associated with the tungsten complexes, suggest that when it is incorporated within a polymer, the M_2 unit will be an excellent harvester of photons and will serve to promote electrons to the conduction band. In this regard, we anticipate that a dimetalated polymer will represent an n-doped semiconductor. Oxidation of the polymer will generate metal centered holes that are strongly coupled to the valence band of the polythiophene. We have found[40] that these model compounds are emissive and, as can be expected from the absorption spectra, the emission occurs well into the near-IR. As yet, no lifetime measurements have been made.

Further studies aimed at incorporating M_2 quadruply bonded units into polythiophenes are underway.

Acknowledgment. We thank the National Science Foundation for financial support and the Ohio Supercomputer Center for computational resources. Professor Jeffrey M. Zaleski and Mr. David F. Dye are thanked for their help in obtaining the low-temperature UV−vis spectra. Mr. Brian D. Pate is also acknowledged for obtaining the EPR spectra.

Supporting Information Available: CIF file for the crystal structure $Mo_2(O_2C\text{-}2\text{-}Th)_4 \cdot 2THF$ and movie file. This material is available free of charge via the Internet at http://pubs.acs.org.

IC040086N

(40) Byrnes, M. J.; Chisholm, M. H. Unpublished results.